The EMBO Journal vol.9 no.3 pp.631 - 639, 1990

Intracellular transport of soluble and membrane-bound glycoproteins: folding, assembly and secretion of anchor-free influenza hemagglutinin

Ila Singh, Robert W.Doms[1], Krystn R.Wagner[2] and Ari Helenius

Department of Cell Biology, Yale University School of Medicine, 333 Cedar Street, New Haven, CT 06510, USA

[1]Present address: NIH, Laboratory of Pathology, Bldg. 10, Rm 2N212, Bethesda, MD 20892, USA

[2]Present address: US Agency for International Development S&T/H/AIDS, Rm 709, Bldg. SA-18, Washington DC 20523, USA

Communicated by J.J.Skehel

The influenza hemagglutinin precursor (HA0) and many other glycoproteins fold and oligomerize in the endoplasmic reticulum (ER). Only correctly folded oligomers are transported to the cell surface. To analyse the rules which determine this type of ER sorting, we have extended our analysis of hemagglutinin transport to two soluble, anchor-free recombinant HA0s derived from X31/A/Aichi/68 and A/Japan/305/57 influenza A. The results showed that individual monomers rapidly acquired a folded structure similar to that of monomeric membrane-anchored HA0. They were efficiently transported and secreted, but oligomerization was not required for secretion. Trimers or higher order complexes were either not formed (X31 HA0), or appeared during passage through the late compartments of the secretory pathway, with no effect on the rate of transport (Japan HA0). However, when initial folding was disturbed by inhibition of N-linked glycosylation, anchor-free X31 HA0 was misfolded and retained in the ER as disulfide-linked complexes associated with binding protein, BiP (GRP78). The complexes were similar to those seen for the non-glycosylated membrane-bound HA0, but instead of forming immediately after synthesis they appeared with a half-time of 6 min. Taken together, the data demonstrate that the structural criteria that makes the anchor-free HA0 transport competent are less stringent than those for the membrane form; they must fold correctly but do not need to oligomerize.

Key words: anchor-free glycoprotein/BiP/endoplasmic reticulum/influenza hemagglutinin/intracellular transport/oligomerization

Introduction

A correct tertiary and quaternary structure is required to make most membrane glycoproteins and many soluble secretory proteins competent for transport out of the endoplasmic reticulum (ER) (Carlin and Merlie, 1986; Gething and Sambrook, 1989; Hurtley and Helenius, 1989; Rose and Doms, 1988). Proteins which fail to fold or assemble correctly arise continuously as side-products during normal biosynthesis. These are generally retained in the ER and eventually degraded. By limiting secretion and surface expression in this way, the ER imposes a remarkable degree of 'quality control' which may be crucial for cellular function.

Much of what is known about conformation-specific sorting in the ER has been learned from two viral proteins; the influenza hemagglutinin precursor (HA0) and the vesicular stomatitis virus G protein. Both are homotrimeric, non-covalently associated transmembrane proteins with acid-triggered membrane fusion activity. Once translocated into the ER, the individual glycopolypeptides fold and acquire their full complement of disulfide bonds in 1–4 min (Machamer *et al.*, 1989; H.Hoover-Litty and A.Helenius, unpublished observations). Trimerization follows with a half-time of 7–10 min after completed synthesis (Copeland *et al.*, 1986; Gething *et al.*, 1986; Machamer *et al.*, 1989; Yewdell *et al.*, 1988). The trimers are rapidly transported to the Golgi complex and reach the plasma membrane with a half-time of 30 min.

In order to exit the ER, membrane-bound HA0 and G protein are subjected to at least three types of structural restrictions: (i) The ectodomain of the individual subunits must fold correctly. Misfolding can be artifically induced by inhibition of N-linked glycosylation by tunicamycin, or by introducing mutations in ectodomains of the HA0 and G proteins. Misfolded proteins are aggregated and sometimes cross-linked by disulfide bonds (Hurtley *et al.*, 1989; Machamer and Rose, 1988). They associate with binding protein (BiP, also called GRP78), a heat-shock related soluble protein in the ER lumen (Copeland *et al.*, 1986; Gething *et al.*, 1986; Hurtley *et al.*, 1989; Machamer *et al.*, 1989). (ii) The cytoplasmic domain must also fulfill structural requirements. Deletions and extensions in the C-terminal cytoplasmic domain can inhibit transport of HA0 and G protein without necessarily affecting the folding and trimerization of the lumenal domains (see Gething *et al.*, 1989; Rose and Doms, 1988). In these cases the retained proteins generally do not bind BiP. (iii) The proteins must oligomerize. Unassembled monomers are not efficiently transported. They do not aggregate in the ER, nor do they stably associate with BiP (Copeland *et al.*, 1986; Doms *et al.*, 1987). While these rules are generally applicable to membrane proteins, it is not known if secretory proteins need to meet all these requirements. That less stringent structural requirements might apply for soluble proteins, has been suggested by observations on proteins such as β_2-microglobulin of MHC Class I antigens, the light chain of immunoglobulin and a variety of secretory proteins which can be secreted as monomers. Other examples, such as procollagens, fibrinogen, the β chain of lutenizing hormone, the heavy chain of IgG and the A and B chains of platelet-derived growth factor (PDGF) suggest that soluble proteins may also need to acquire the appropriate quaternary structure before efficient release from the ER (for reviews see Carlin and Merlie, 1986; Hurtley and Helenius, 1989).

By comparing the same protein, influenza HA0, in membrane-bound and soluble forms, it was possible to test rigorously if secretory proteins are subject to the same conformational control as membrane proteins. Gething and Sambrook (1982) demonstrated that anchor-free HA0 is efficiently secreted when expressed in tissue culture cells. On the basis of chemical cross-linking, they suggested that the secreted anchor-free HA0 are trimers. We have extended these studies here and show that, depending on the strain and construct used, the secreted HA0 is either monomeric, trimeric or aggregated. To be transported from the ER, the soluble HA0 monomers must fold correctly but they do not need to trimerize. Trimerization and aggregation—when they occur—are late events. These results illuminate some of the basic rules involved in ER quality control.

Results

Rates of transport and secretion

We first determined the kinetics and efficiency by which anchored and anchor-free HA0 (A^+HA0 and A^-HA0, for short) were transported through the secretory pathway. Hemagglutinins from two different influenza strains were used: A/Japan/305/57 (subtype H2) and the recombinant X31/A/Aichi/68 (subtype H3). The proteins were expressed in CV-1 cells using SV40-HA recombinant viruses developed and characterized by Gething and Sambrook (1982) and Doyle *et al.* (1986). After 48 h of infection, the cells were pulse-labeled with [^{35}S]methionine for 5 min and chased for variable times in the presence of cold methionine. To monitor secretion of A^-HA0, the overlying medium was collected. The medium and cell lysates were immunoprecipitated with polyclonal antibodies to hemagglutinin (HA). A portion of each precipitate was digested with endoglycosidase H (Endo H) to determine which fraction of the HA0 possessed Endo H resistant N-linked oligosaccharides. Acquisition of Endo H resistance is commonly used to monitor glycoprotein passage into the medial Golgi and subsequent compartments in the pathway (Kornfeld and Kornfeld, 1985). The immunoprecipitates of the various samples were analyzed by SDS−PAGE, fluorography and quantitated by densitometry.

The results shown in Figure 1A confirmed the previous finding of Gething and Sambrook (1982) that the A^-HA0 is efficiently secreted. Compared to the A^+HA0s, of which only 65−80% reach the medial Golgi and the cell surface (Figure 1A, see also Copeland *et al.*, 1986), secretion of

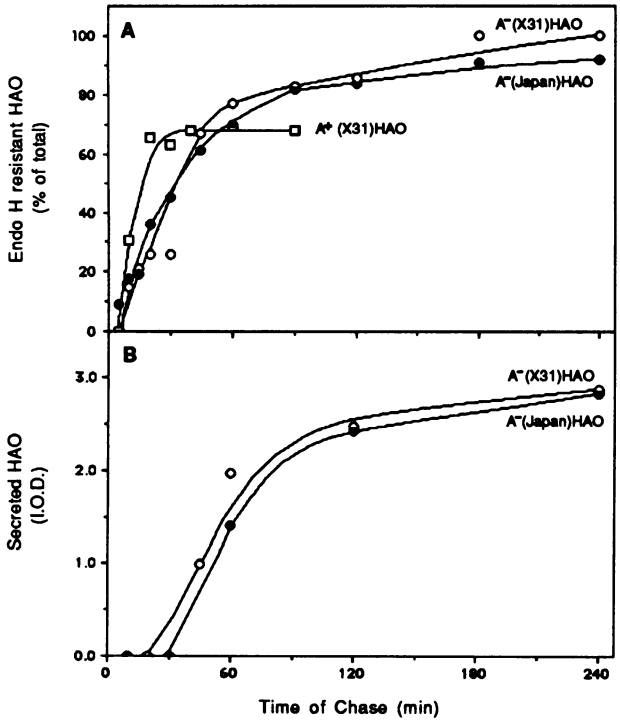

Fig. 1. Kinetics of A^+ and A^-HA0 transport and secretion. CV-1 cells expressing A^-(X31)HA0, A^-(Japan)HA0 or A^+(X31)HA0 were labeled for 5 min with [^{35}S]methionine, and chased for the indicated times. Fractions of the medium and cell lysates were immunoprecipitated with polyclonal anti-HA serum. For A, aliquots of the precipitated HA0 were treated with Endo H. The samples were analysed by SDS−PAGE and fluorography. The HA0 bands, quantitated by densitometry, are expressed as integrated optical density units (I.O.D.), or as percent of total precipitable HA0. (**A**) The acquisition of Endo H resistance of A^-(Japan)HA0 [●−●], A^-(X31)HA0 [○−○] and A^+(X31)HA0 [□−□]. (**B**) The secretion of A^-(Japan)HA0 [●−●] and A^-(X31)HA0 [○−○] into the medium.

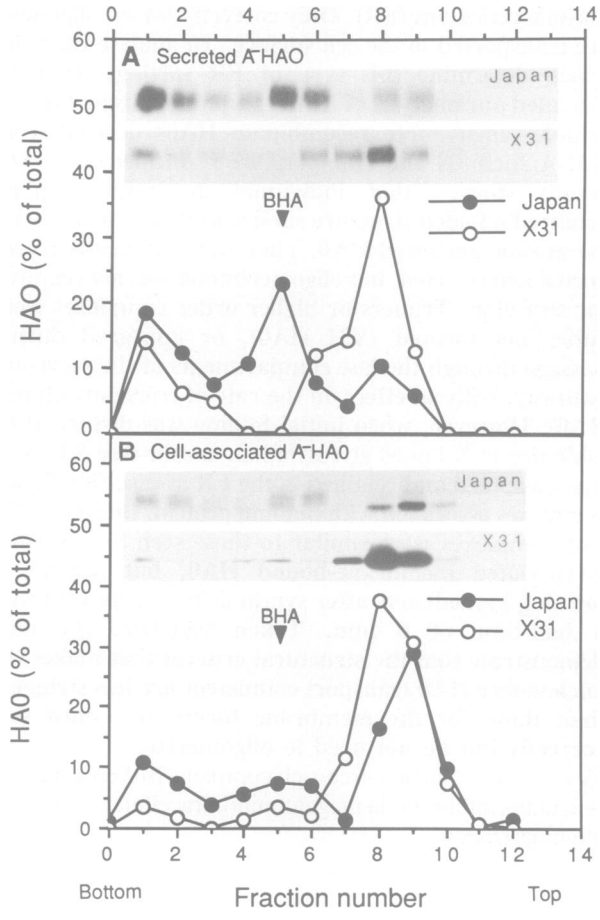

Fig. 2. Velocity sedimentation of A^-HA0 on continuous sucrose gradients. Cells expressing A^-HA0 were pulsed for 5 min with [^{35}S]methionine followed by either a 1 h chase [A^-(X31)HA0] or a 2 h chase [A^-(Japan)HA0]. The medium and cell lysates were centrifuged on 5−20% (w/v) sucrose gradients containing 0.1% Triton X100. Each fraction was immunoprecipitated, analysed by SDS−PAGE and quantitated by densitometry. (**A**) A^-(Japan)HA0 [●−●] and A^-(X31)HA0 [○−○] in the medium. The inserts show the SDS−PAGE of the A^-HA0 in the different gradient fractions, and the graph depicts the quantitation by densitometry. (**B**) Cell associated A^-(X31)HA0 and A^-(Japan)HA0. The trimeric bromelain fragment of HA (BHA, 8.9S) (Brand *et al.*, 1972) was used as a standard in parallel gradients.

both A⁻HA0s was very efficient (>90%). It is also apparent from Figures 1A and B (see also Gething and Sambrook, 1982; Copeland *et al.*, 1986) that the A⁻HA0s were transported with slower kinetics than A⁺HA0. Arrival at the medial Golgi occurred with a $t_{1/2}$ of 35 min instead of 15 min, and secretion occurred with a $t_{1/2}$ of 60 min instead of 30 min (see Copeland *et al.*, 1986). It is noteworthy that A⁻HA0s were transported more slowly than their A⁺ counterparts not only from the ER to the Golgi, but also from the Golgi to the plasma membrane.

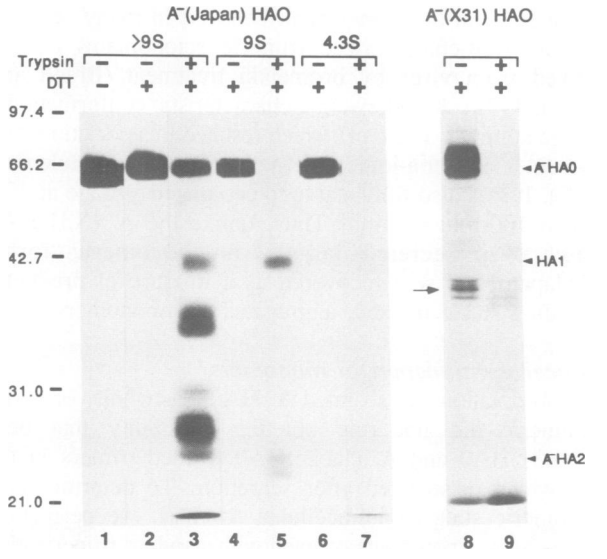

Fig. 3. Effect of trypsin on A⁻HA0. Secreted A⁻(Japan)HA0 was sedimented as in Figure 2A. Peak fractions were digested with trypsin. The trypsin was inactivated with soybean trypsin inhibitor, and the HA0 immunoprecipitated with a polyclonal anti-HA antibody, reduced with dithiothreitol (DTT) and analysed by SDS–PAGE. The arrowheads indicate the positions of A⁻HA0, HA1 and A⁻HA2. The material denoted 4.3S represents monomers, 9S represents trimers and >9S aggregates of A⁻(Japan)HA0. The A⁻(X31)HA0 used, represented unfractionated secreted and cell-associated HA0. Numbers of the left indicate mol. wt in kd. The arrow shows background bands corresponding to SV40-VP1.

Secreted A⁻(X31) HA0 is monomeric

Trimer formation can be monitored by velocity sedimentation and by immunoprecipitation with trimer-specific monoclonal anti-HA antibodies (Copeland *et al.*, 1986; Gething *et al.*, 1986; Yewdell *et al.*, 1988). Also, trimeric HA0 is resistant to digestion with trypsin, save for the activating cleavage of HA0 which produces the disulfide-linked subunits HA1 and HA2, while monomeric and misfolded forms are digested to acid-soluble fragments (Copeland *et al.*, 1986; Gething *et al.*, 1986). We used these assays to examine the oligomeric state of secreted A⁻(X31)HA0 and A⁻(Japan)HA0.

All three assays showed that the majority of secreted A⁻(X31)HA0 was monomeric. As seen in Figure 2a, most of it sedimented as a single peak in sucrose velocity gradients with a sedimentation coefficient corresponding to the monomeric form of HA0 (4.3S, Copeland *et al.*, 1986; Doms and Helenius, 1986). The same result was obtained whether the non-ionic detergent Triton X-100 (TX100) was included in the gradient or not. Less than 5% of the HA0 was consistently recovered from fractions corresponding to 9S trimers, while 10–20% of the HA0 formed even larger assemblies. Moreover, all of the secreted HA0 was sensitive to trypsin digestion (Figure 3, lanes 8 and 9). Finally, no detectable A⁻(X31)HA0 was precipitated from the medium by the trimer-specific antibodies N1 and N2 (Table I).

When the conformation of the monomeric A⁻(X31)HA0 was further analysed with a panel of conformation-specific monoclonal antibodies, it was found to be similar to monomeric A⁺HA0. While it was non-reactive with antibodies that precipitate trimeric HA0, it reacted with a

Table I. Precipitation of glycosylated and non-glycosylated A⁻(X31)HA0 with conformation specific monoclonal antibodies[a]

Antibody	Antigen		Reference
	A⁻(X31)HA0	A⁻(X31)HA0(+TM)[d]	
Reactive with acid-treated/misfolded HA0:			
A1 (HA2)[b]	+	++	1[c]
A2 (HA1)	–	++	1
H26D08 (HA1; aa 98–106)	+/–	++	2
Trimer specific:			
N2 (Site B)	–	–	1
N1 (Site B)	–	–	1
HC110 (Site B; aa 189)	–	–	3
Top domain specific:			
HC159 (Site A; aa 143)	+	+	4
HC3 (Site A; aa 144)	++	+	4, 5
HC19 (Site B; aa 157)	+	+	4, 5
HC68 (Site B; aa 193)	+/–	–	4
HC125 (Site B; aa 199)	+/–	–	3
HC31 (Site B; aa 198)	+	+	5
HC100 (Site E; aa 63)	++	+	4

[a]CV-1 cells expressing A⁻(X31)HA0 were pre-treated with medium containing 5 μg/ml tunicamycin or with tunicamycin-free medium for 1 h, pulsed for 10 min with [^{35}S]methionine and chased for 60 min. Cells were lysed, combined with medium and precipitated with a polyclonal anti-HA antibody and with monoclonal antibodies as described in Materials and methods.

[b]The brackets provide information about the location of the epitopes, the amino acid residues (aa) involved and the subunit of HA0. All antibodies, except A1, were against epitopes in the HA1 subunit.

[c]The references are 1, (Copeland *et al.*, 1986); 2 (Wilson *et al.*, 1984); 3, (Daniels *et al.*, 1987); 4, (Daniels *et al.*, 1984); and 5, (Daniels *et al.*, 1983).

[d]TM = tunicamycin, 5 μg/ml (see Materials and methods).

variety of monoclonals obtained from Dr John Skehel which bind to epitopes in the top HA1 domain (Table I, Daniels *et al.*, 1983, 1984, 1987). We have previously reported that these antibodies are indeed conformation specific, as they do not precipitate denatured HA0 (Copeland *et al.*, 1988; Hurtley *et al.*, 1989). A^-(X31)HA0 was also not precipitated with monoclonal A2 which recognizes the misfolded conformation acquired after tunicamycin treatment (Table I, Copeland *et al.*, 1986; Hurtley *et al.*, 1989). Some of the protein reacted with H26D08 (Wilson *et al.*, 1984), an anti-peptide monoclonal which binds an epitope buried in the HA1 trimer interface. When taken together with the observation that monoclonal A1, which sees A^+(X31)HA0 only after misfolding (Copeland *et al.*, 1988), reacted with ~50% of the secreted A^-(X31)HA0 (Table I), this indicated that some of the secreted protein was aberrantly folded (Doms *et al.*, 1985). We concluded that 80% or more of the secreted A^-(X31)HA0 was monomeric and that its conformation was similar but not completely identical to ER-restricted monomers of the A^+HA0.

Secreted A^-(Japan) HA0 is present as monomers, trimers and aggregates

When the secreted A^-(Japan)HA0 was subjected to velocity sedimentation, three peaks were seen (Figure 2a). They corresponded to monomers (4.3S), trimers (9S) and aggregates (>9S) (Doms and Helenius, 1986). The distribution suggested that the majority of the HA0 had oligomerized. When the HA0 present in each peak was analysed by trypsin digestion (Figure 3a), a differential sensitivity was observed. While the monomers in the 4.3S peak were almost completely degraded (Figure 3, lanes 6 and 7), the HA0 present in the trimer peak was resistant in as far as it could only be cleaved to HA1 and A^-HA2 (lanes 4 and 5). The HA0 in the aggregated peak gave a mixed pattern of fragments which, in addition to some non-digested A^-HA0, included HA1, A^-HA2 as well as bands at 40 kd and 27 kd (lane 3). Non-reducing gels revealed that the aggregates were not disulfide linked (lane 1).

The HA0 in the trimer peak behaved in many respects like the well-characterized trimeric ectodomains of HA derived from virus by bromelain treatment (Brand and Skehel, 1972). It underwent a characteristic conformational change at mildly acidic pH which resulted in association with liposomes and non-ionic detergents (Doms and Helenius, 1988). It was also fully stable to prolonged storage at 4°C and to 100-fold dilution. Thus, unlike the A^-(X31)HA0 which was secreted largely in monomeric form, A^-(Japan)HA0 was recovered as a mixture of products, including stable trimers, aggregates and monomers.

Intracellular transport of monomers

The observation that secreted A^-HA0 was wholly or partly monmeric did not rule out the possibility that both A^-(X31)HA0 and A^-(Japan)HA0 formed trimers in the cell which dissociated after secretion. To determine the oligomeric state of intracellular A^-HA0, we performed pulse-chase experiments coupled with standard trimerization assays. When analysed on velocity gradients, the intracellular A^-(X31)HA0 was found to be largely monomeric at all times of chase (see Figure 2b, for 1 h chase). It could not be precipitated from pulsed cell lysates using the trimer-specific monoclonals N1 and N2, nor could trypsin resistant A^-(X31)HA0 be detected at any time of chase (Figure 3, lanes 8 and 9). The results suggested that A^-(X31)HA0

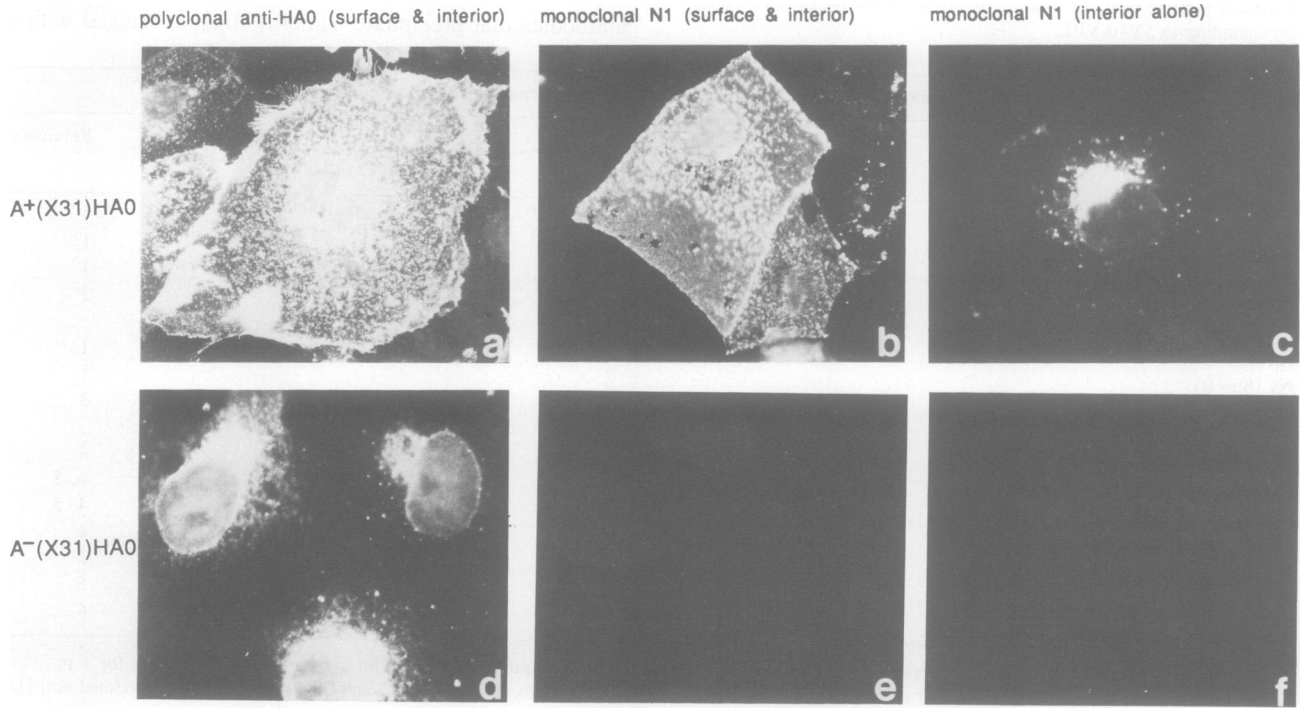

Fig. 4. Distribution of total and trimeric HA0 in cells expressing A^+(X31)HA0 and A^-(X31)HA0. HA0 was visualized by indirect immunofluorescence using either a polyclonal anti-HA antibody (which sees all forms of HA and HA0) or monoclonal N1 (which is trimer specific). **a**, **b** and **c** expressed A^+(X31)HA0; **d**, **e** and **f** expressed A^-(X31)HA0. **a** and **d** were stained with the polyclonal antibodies after fixation and permeabilization, **b** and **c** with N1. **c** and **f** were first treated with acidic buffer which converted the cell surface HA0 to a form not detected with N1, whereafter the cells were permeabilized to expose internal HA0.

remained monomeric throughout the biosynthetic pathway.

Since it was possible that intracellular oligomers were present in the cell, but were dissociated by the non-ionic detergent, we prepared detergent-free cell lysates from pulse-labeled cells by sonication. Velocity sedimentation was then performed in the absence of detergents. The results were no different from those in the presence of TX100, i.e. the majority of HA0 sedimented as monomers (cf. Figure 2b). We also performed indirect immunofluorescence on fixed cells using the trimer-specific monoclonal antibody N1 and polyclonal anti-HA antibody (Figure 4). Whereas N1 stained trimers could easily be demonstrated on the cell surface, in the ER and in the Golgi complex of cells expressing A^+(X31)HA0 [Figure 4, b and c], we found no staining in cells expressing A^-(X31)HA0 [Figure 4, e and f]. The intracellular A^-(X31)HA0 in these cells could be easily visualized, however, in the Golgi complex using the polyclonal anti-HA antibodies which do not distinguish between monomers and trimers [Figure 4d]. We concluded that A^-(X31)HA0 was present in monomeric form throughout the secretory pathway, and that it was able to exit the ER and be secreted without first forming a trimer.

When A^-(Japan)HA0 was subjected to velocity sedimentation, the intracellular forms were also found to be predominantly monomeric (Figure 2b). Intracellular trimers and aggregates appeared only late in the secretory pathway, with a half-time of formation of ~50 min (Figure 5). The same kinetics were observed for acquisition of trypsin resistance (not shown). Since oligomerization and aggregation of A^-(Japan)HA0 occurred after or coincident with acquisition of Endo H resistance (cf. Figure 1A and B), formation of stable trimers must have taken place in the medial Golgi or before arrival at the cell surface. As trimerization and aggregation coincided, it is possible that the aggregates were made up of trimeric HA0 units. This was consistent with the presence of HA1 and A^-HA2 subunits on trypsin treatment of the aggregates.

Taken together, the results indicated that, in contrast to their membrane-anchored analogs, both A^-(X31)HA0 and A^-(Japan)HA0 were transported from the ER to the Golgi as monomers. Whereas A^-(X31)HA0 continued to the cell surface in monomeric form, a large fraction of A^-(Japan)HA0 formed stable trimers and aggregates as it passed through the medial- and trans-Golgi compartments or the secretory vesicles. The rate of secretion was not dependent on whether the proteins were trimers and aggregates or monomers (data not shown), suggesting that they were secreted by the same pathway without being separated.

Retention of misfolded A^-(X31)HA0

Since oligomeric assembly was not required for the intracellular transport of soluble anchor-free HA0, it was of interest to determine whether the requirement for correct initial folding, demonstrated by anchored HA0, was also waived. It has been previously shown that A^+(X31)HA0, like many other glycoproteins, cannot fold correctly if N-linked glycosylation is inhibited by tunicamycin (Hurtley *et al.*, 1989). It gets cross-linked immediately after synthesis through aberrant interchain disulfides. It associates with BiP and remains in the ER. While the top domain seems correctly folded under these conditions, the stem domain is misfolded as evidenced by exposure of an epitope that is not present in correctly folded trimers.

The fate of non-glycosylated A^-(X31)HA0 in tunicamycin-treated cells was found to be quite similar. It remained restricted to an organelle with a reticular morphology corresponding to that of the ER (Figure 6) and it was not secreted (Figure 7, lanes 2: 1 h chase; and lane 3: 4 h chase). SDS–PAGE of reduced and non-reduced samples showed that it was present as disulfide cross-linked aggregates (Figure 7, lanes 6 and 7). On sucrose velocity gradients it behaved as a heterogeneous mixture of aggregates with sedimentation coefficients in the 9–25S range (Figure 8). Co-precipitating with the HA0, particularly in the larger aggregates, was a labeled protein of 78 kd which we have previously identified as BiP (Figure 9, insert; Hurtley *et al.*, 1989). Indeed, when the cell lysates were subjected to immunoprecipitation with a monoclonal to BiP, a large

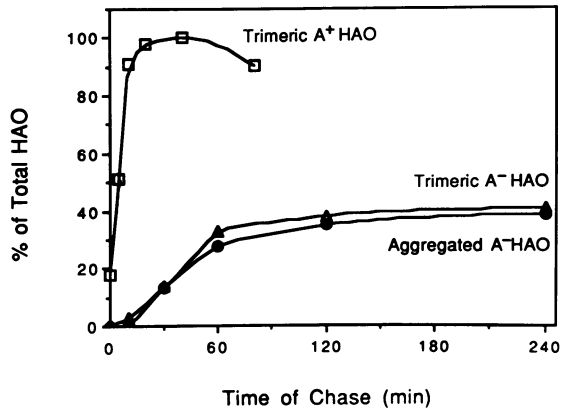

Fig. 5. Oligomerization and aggregation kinetics for A^-(Japan)HA0. Cells expressing A^-(Japan)HA0 were pulsed for 5 min with [^{35}S]methionine, and chased for the indicated times. Medium and cell lysates were subjected to velocity sedimentation, immunoprecipitation and SDS–PAGE analysis as in Figure 2. The fraction of HA0 precipitable in trimer and aggregate peaks was quantitated by densitometry. The kinetics of trimerization for A^+(X31)HA0 has been included from Copeland *et al.* (1986) for comparison. The trimer A^+(X31)HA0 and A^-(Japan)HA0 have previously been shown to be identical in this system (Copeland *et al.*, 1986; Gething *et al.*, 1986).

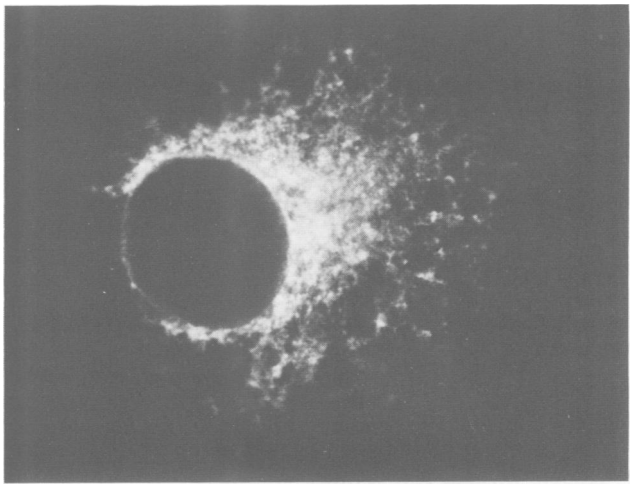

Fig. 6. Intracellular distribution of A^-(X31)HA0 in cells treated with tunicamycin. Forty six hours after infection with the recombinant SV40 virus expressing A^-(X31)HA0, tunicamycin 5 μg/ml was added. After a further 3 h, cells were fixed and permeabilized. Indirect immunofluorescence was performed using polyclonal anti-HA. The reticular staining seen is typical for the ER.

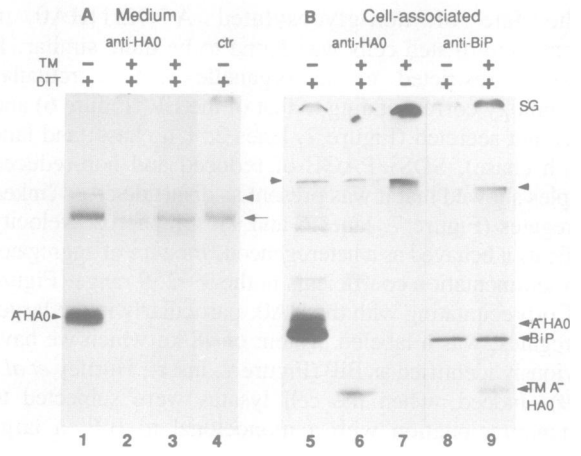

Fig. 7. Properties of non-glycosylated A^-(X31)HA0. Forty six hours post-infection, cells expressing A^-(X31)HA0 were treated with 5 μg/ml tunicamycin (TM) for 1 h. They were pulsed for 10 min, and chased for 1–4 h. The medium and cell lysates were immunoprecipitated with polyclonal anti-HA, monoclonal anti-BiP or with control antibodies. Samples were subjected to SDS–PAGE with or without prior reduction with DTT. (**A**) The medium, **lane 1**: noTM, 1 h chase; **lane 2**: TM+, 1 h chase; **lane 3**: TM+, 4 h chase; **lane 4**: control antibody (**B**). The cell lysate. All lanes show the 1 h chase time. The arrow heads indicate the interface between the stacking and separation gels. SG stands for the top of the stacking gel. The arrow marks a non-specific background band, also seen on immunoprecipitation with a control antibody (**lane 4**). TM treatment causes a partial inhibition of HA0 synthesis, which explains why there is less labeled HA0 in **lane 6** than in **lane 5**.

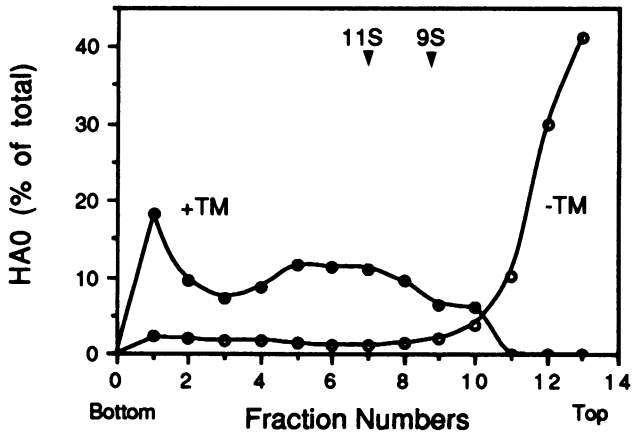

Fig. 8. The size distribution of aggregated non-glycosylated A^-(X31)HA0. Sedimentation of A^-(X31)HA0 synthesized in the presence [●–●] or absence [○–○] of tunicamycin. Cells treated with tunicamycin as in Figure 7 (or treated with the DMSO solvent alone), were lysed and centrifuged on sucrose velocity gradients as in Figure 8 except that the run was much shorter (for details, see Materials and methods). Monomers sediment in the top three fractions. Catalase (11S) and BHA (9S) were used as size markers. The bottom of the gradient corresponds to 25S.

fraction (40%) of the HA0 was co-precipitated (Figure 7, lane 9).

It has been previously shown that the BiP-associated aggregates of non-glycosylated A^+(X31)HA0 form within 1–3 min of synthesis (Hurtley *et al.*, 1989). Velocity sedimentation of samples obtained after pulse and chase showed that the A^-(X31)HA0 complexes formed somewhat more slowly (Figure 9A and B). The majority of A^-(X31)HA0 labeled during a 2 min pulse sedimented as

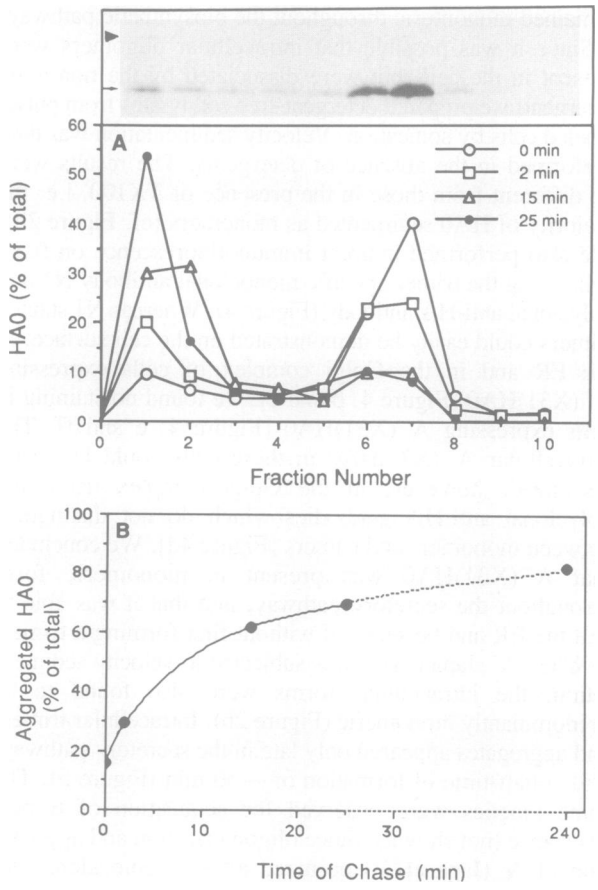

Fig. 9. Kinetics of aggregation of non-glycosylated A^-(X31)HA0. Cells treated with tunicamycin as in Figure 7 were pulsed with [^{35}S]methionine for 2 min, and chased for 0 [○–○], 2 [□–□], 15 [△–△] and 25 [●–●] min. Cell lysates were centrifuged, immunoprecipitated and quantitated as in Figure 2. Monomers sediment in fraction 6 and 7, trimers in fraction 4 and aggregates in fractions 1 and 2 (see Figure 2). **Insert** shows the gel corresponding to the 2 min chase time. (**B**) amount of aggregate (non-glycosylated HA0 in fractions 1 and 2 of gradients shown in **A**) at different times of chase.

monomers immediately after the pulse (see insert in Figure 9). A more complete time course showed that the aggregates appeared with a $t_{1/2}$ of 6 min after synthesis (Figure 9B). Similar kinetics were observed for expression of the A1 epitope and for interchain disulfide cross-linking (not shown). It is conceivable that this difference in the rate of aggregation of anchor-free HA0, compared to anchored HA0, is due to the reaction occurring in free solution rather than in the lateral plane of the ER membrane.

The non-glycosylated HA0 remained sensitive to trypsin (not shown). It also reacted with monoclonal antibodies specific for misfolded HA and HA0 (Table I), was precipitated by several of the monoclonals to the top domain, but was not recognized by the trimer-specific antibodies (Table I).

The results demonstrated that the anchor-free molecules were retained in the ER as misfolded, disulfide-linked aggregates associated with BiP. Their conformation was similar to that of non-glycosylated and misfolded A^+(X31)HA0. These findings indicated that the requirement for correct folding applied equally to the intracellular transport of both A^+ and A^-HA0.

Discussion

Soluble and membrane-bound proteins are transported together in the secretory pathway. They pass through the same organelles, they undergo similar post-translational modifications and they are subject to similar regulation and sorting (Palade, 1975). As extensively discussed in recent reviews (Burgess and Kelly, 1989; Klausner, 1989; Pfeffer and Rothman, 1987; Rose and Doms, 1988), one principal difference between the transport of soluble proteins and membrane proteins is that the former may move as part of the bulk fluid flow while the latter may follow a bulk outward flow of membrane. Since the membrane/volume ratios vary in the different organelles and vesicles of the pathway, the bulk rates of transport of soluble and membrane-bound molecules need not necessarily be the same. It is not unexpected to find, as was the case of A^-HA0 and A^+HA0 (see Figure 1; Gething and Sambrook, 1982), that transport from the ER to the Golgi and from the Golgi to the plasma membrane takes more time for the anchor-free than the anchored molecule (Strous and Lodish, 1980).

Superimposed on the non-selective bulk traffic are mechanisms which alter transport rates of individual protein species. They may cause retention, segregation (at branching points of the pathway) or perhaps acceleration over and beyond the bulk rates. Differences in kinetics and efficiency observed in secretion of proteins (Fitting and Kabat, 1982; Lodish *et al.*, 1983) suggests that modulation of this type is common, and that it is the exit from the ER that generally constitutes the rate limiting step.

Since the rules for transport need not be the same for soluble and membrane-bound proteins, it was of interest to compare the effects of folding and oligomerization for the same protein in the two forms. Influenza HA is one of the few membrane glycoproteins for which detailed three-dimensional data is available. The crystal structure of the bromelain-released ectodomain fragment (Wilson *et al.*, 1981; Wiley and Skehel, 1987) reveals a 13.5 nm long homotrimeric spike with large contact areas between neighboring subunits. The fact that these trimers are stable demonstrates that the anchor is not necessary for the quarternary structure and suggests that ectodomains alone may contain enough structural information to allow trimerization. Indeed, the finding that stable and structurally intact trimers can be formed from the A^-(Japan)HA0 (Figure 2) confirms this notion. While the role of the topological domains during A^+HA0 trimerization in the ER is unclear, it is definitely possible that assembly is initiated through specific interactions between the ectodomains. In the final trimers however, the anchors contribute to overall stability (Doms and Helenius, 1986).

Our results indicated that A^-HA0, in contrast to A^+HA0, did not need to trimerize in order to be transported and secreted. Intracellular and secreted A^-(X31)HA0 was largely monomeric, both in the presence and absence of non-ionic detergent. A^-(Japan)HA0, while largely oligomeric in its secreted form, also appeared to exit the ER as monomers. Trimerization and aggregation occurred after the protein had become endo H resistant, i.e. in the Golgi complex or in secretory vesicles. The apparent difference between transport requirements can probably be understood as a difference in retention; membrane-bound monomers are efficiently retained in the ER, while monomers in solution are not. The observation that the conformation of the secreted A^-HA0 was similar to the ectodomain of A^+HA0 monomers prior to trimerization, suggested that the 'signal' for retention is in the transmembrane and/or the cytoplasmic domains. This is consistent with observations on HA0 and VSV G-protein mutants which show that defects in the cytoplasmic domain can lead to ER retention without necessarily affecting the trimerization or the conformation of the cytosolic domains (Doms *et al.*, 1988; Gething *et al.*, 1986).

The heterogeneous non-covalent aggregates observed in the secreted A^-(Japan)HA0 were interesting in several respects. Formed late in the secretory pathway, their conformation was slightly misfolded as judged by their partial sensitivity to trypsin. The aggregates did not seem to contain other protein components. Aggregation could be triggered by the increased concentration of HA0 in the Golgi (Copeland *et al.*, 1988) an by the lower pH in the trans Golgi compartment (Anderson and Pathak, 1985; Schwartz *et al.*, 1985). On the other hand, it could also depend on the addition of sialic acid to the complex oligosaccharide side chains of the HA0 which occurs in the trans Golgi, and the subsequent agglutination of HA0s through their receptor binding sites. This possibility is suggested by Dr Geert Maertens who finds that similar aggregates in A^-HA0 of the Victoria strain can be dissociated into trimers by exhaustive neuraminidase treatment (personal communication). Skibbens *et al.* (1989) have recently reported that a large fraction of the A^+HA0 in influenza-infected cells enters an insoluble aggregate in the trans Golgi, and that intrachain disulfides are modified. While this is not a major fraction in A^+HA0 when expressed in CV-1 cells (see Figure 1a), it may be related to the formation of aggregates of A^-(Japan)HA0.

The difference between the X31 and Japan A^-HA0 with respect to assembly may depend on the strain difference. Hemagglutinins from the HA2 and HA3 subtypes of influenza A display many differences. Another reason for the difference may be the presence of a point mutation (HA1 266 Ser to Leu) in the A^-(X31)HA0 cDNA (I.Singh, unpublished result). We first found this mutation in a recombinant virus expressing A^+(X31)HA0 (Doyle *et al.*, 1986; Wagner and Helenius, in preparation). Inadvertently, but advantageously for this study, the mutation is located in the interface between the head and the stem domains. While this mutation does not inhibit trimerization of A^+(X31)HA0 and trimers can be detected by trimer-specific antibodies, it makes them unstable to velocity sedimentation in the presence of TX100. It is conceivable therefore, that this mutation may make the A^-HA0 molecule incapable of forming trimers. Whatever the reasons for its lack of trimerization, the A^-(X31)HA0 was useful in this study as it illustrated the lack of an assembly requirement for the transport of A^-HA0.

The results obtained with tunicamycin demonstrated that non-glycosylated A^-(X31)HA0 was transport incompetent. The retention involved aggregation, formation of interchain disulfides and association with BiP. The top domain epitopes were relatively intact, and the aberrant epitope in HA2 for monoclonal antibody A1 was expressed. The only difference in the fate of non-glycosylated A^-(X31)HA0 and A^+(X31)HA0, which we have studied previously (Hurtley *et al.*, 1989), was that the retention complexes formed at

different rates: whereas the aggregate of A^+(X31)HA0 appears with a $t_{1/2}$ of 1–3 min, the $t_{1/2}$ of aggregation of A^-(X31)HA0 was 6 min. This may indicate that, whereas the misfolded membrane-bound HA0 associates laterally in the membrane immediately after release from the polysome, the complexes of soluble HA0 are released into the lumen of the ER before aggregation and BiP association can occur. Such a mechanism would be consistent with studies on pancreatic cells where the formation of massive, disulfide-linked aggregates of misfolded zymogens can be induced in the ER lumen (Palade, 1956; Tooze *et al.*, 1989).

So far, very little is known about the molecular events underlying conformation dependent sorting events in the ER which provide selective transport of correctly structured proteins. Taken together, our results demonstrate that HA0 molecules undergo at least two independent 'quality control' steps: one which requires correct folding of the subunit polypeptides, and another which requires correct oligomerization. The two events are independent of each other, as only the former applies to the soluble anchor-free HA0.

Materials and methods

Cells and recombinant virus vectors

CV-1 monkey kidney cells were grown as described earlier (Doxsey *et al.*, 1985). SV40 late replacement vectors used for the expression of anchored and anchor-free HA were provided by Drs C.Doyle, J.Sambrook and M.-J.Gething. SVEHA20A^- lacked 38 amino acids from the C terminus of HA derived from the A/Japan/305/57 (H2) strain of influenza virus. This deletion included the hydrophobic anchoring sequence and the cytoplasmic tail (Gething and Sambrook, 1982). The other, SVEXHA-A^-, lacked 35 amino acids from the C terminus of HA derived from a recombinant influenza virus, X-31, in which the HA was from the A/Aichi/68 (H3) strain (Doyle *et al.*, 1986). In conjunction with a helper virus, these vectors were used to infect CV-1 cells as described previously (Copeland *et al.*, 1986).

Antibodies

Polyclonal anti-HA serum was prepared by immunising rabbits with X-31 or Japan virus and the corresponding bromelain-solubilized HA [BHA] (Doms *et al.*, 1985). Mouse monoclonal antibodies, N1 and N2 which are specific for trimeric X-31 HA and A1 which is specific for acid-treated or misfolded X-31 HA, have been previously characterized (Copeland *et al.*, 1986). Monoclonal antibodies, HC159, HC3, HC19, HC68, HC125, HC110, HC100 and HC31, which react with the top domain of X-31 HA0 in a conformation-specific manner were kindly provided by Dr John Skehel (Daniels *et al.*, 1983, 1984, 1987). H26D08 was a gift of Dr Ian Wilson (Wilson *et al.*, 1984). Monoclonal antibody recognizing BiP (Bole *et al.*, 1986) was a gift of Dr David Bole.

Immunofluorescence

Indirect immunofluorescence was performed essentially as described in Copeland *et al.* (1986). Briefly, cells expressing A^-(X31)HA0 and A^+(X31)HA0 48 h post-infection were fixed with 3% paraformaldehyde and permeabilized with 0.1% TX100. Polyclonal rabbit antisera and trimer-specific mouse monoclonals, N1 and N2 were used as the primary antibodies. Fluorescein isothiocyanate-conjugated goat anti-rabbit or goat anti-mouse $F(ab)_2$ fragment of IgG was used as the secondary antibody. In order to remove trimer-specific staining from the cell surface, so that the cell interior could be visualized using trimer-specific antibodies, some cells were treated with trypsin and low-pH buffer as described in Copeland *et al.* (1986).

To localize the non-glycosylated aggregate of A^-(X31)HA0, cells at 46 h of infection were treated with tunicamycin, 5 μg/ml for 3 h, fixed, permeabilized and stained as above. Polyclonal anti-HA antibody was used as the primary antibody.

Metabolic labeling and pulse-chase protocol

Forty eight hours after infection with SVHA20A^- or SVEXHA A^-, cells were washed and incubated in methionine-free Dulbecco's modified Eagle's medium (DMEM) containing 20 mM HEPES for 15 min at 37°C. Each 65 mm dish of subconfluent cells was pulsed with 0.1 mCi [^{35}S]methionine for 5 min at 37°C. Pulse medium was removed, chase medium (DMEM with 10 mM HEPES, 10% FCS and 25 mM cold methionine) warmed to 37°C was added and cells were chased at 37°C for varied periods of time up to 4 h. At the end of the chase period, the medium was collected. Cells were lysed with ice-cold MNT (20 mM MES, 100 mM NaCl and 30 mM Tris) containing 1% Triton X100, 10 μm chymostatin, 10 μm leupeptin, 10 μm antipain, 10 μm pepstatin and 1 mM phenylmethylsulfonyl fluoride. Samples were centrifuged for 5 min in a Brinkmann centrifuge at 4°C, to sediment intact cells in the medium and nuclei in the cell lysates. These supernatants were loaded onto sucrose gradients or immunoprecipitated with conformation-specific antibodies immediately, or frozen in liquid nitrogen and stored at −20°C,

Velocity gradient sedimentation

For separation of A^-HA0 trimers, monomers and aggregates, and for separation of large aggregates of non-glycosylated A^-HA0 from monomers, continuous gradients of 5–20% w/v sucrose in MNT with 0.1% TX100 were poured over a 0.5 ml cushion of 60% sucrose. A fraction of the labeled cell lysate or supernatant was layered on top of the gradient. Gradients were centrifuged in a Beckman SW55 rotor at 45 000 r.p.m. for 14 h at 4°C. Fractionation was carried out from the bottom of the tube, at 4°C for gradients containing non-glycosylated HA0–BiP complex and at room temperature for all the others. Fractions were immunoprecipitated with polyclonal anti-HA antibodies, analysed by SDS–PAGE, fluorography and quantitated by densitometry. Sedimentation coefficients were determined using BHA and transferrin as markers.

To determine the size of the non-glycosylated A^-(X31)HA0 aggregate, cell lysates from tunicamycin-treated, metabolically labeled cells were applied to continuous gradients of 5–25% w/v sucrose with a 1 ml 60% w/v sucrose cushion and centrifuged in a SW40 Beckman rotor at 30 000 r.p.m. for 20 h at 4°C. Gradients were fractionated and A^-HA0 immunoprecipitated from the fractions as described above. Bromelain digested fragment of HA0-BHA (9S) and catalase (11S) were used as markers.

Immunoprecipitations

Immunoprecipitations were done essentially as described in Copeland *et al.* (1986). Briefly, a Staph A–antibody complex was incubated with the sample in the presence of 0.1% TX100. Complexes were washed twice [0.1% TX100 in MNT for A^-(X31)HA0 and 500 mM NaCl, 100 mM Tris for A^-(Japan)HA0] and resuspended in 10 mM Tris, 1 mM EDTA, pH 6.8. They were heated to 95°C for 5 min in gel sample buffer (200 mM Tris pH 6.8, 3% SDS, 10% glycerol, 1 mM EDTA, 0.004% bromophenol blue ± 20 mM dithiothreitol) and analysed by SDS–PAGE (Laemmli, 1970). Fluorography was performed on salicylate-impregnated gels using Kodak XAR-5 film. Fluorographs were scanned and the integrated optical denisty (I.O.D.) of bands was determined by Visage 2000.

In order to preserve the association between non-glycosylated A^-(X31)HA0 and BiP, care was taken to keep all samples at 4°C during the binding of the antibody and the washing of the immunecomplexes.

Endoglycosidase H digestion

Cells expressing A^-HA0 were metabolically labeled as described above. For each chase time, the supernatant was mixed with the cell lysate, and the HA0 immunoprecipitated with polyclonal rabbit antisera. Immune complexes were resuspended in 100 mM sodium acetate pH 5.5 containing 0.2% SDS and boiled for 3 min. An equal amount of 100 mM sodium acetate pH 5.5 was then added. 0.5 U of endoglycosidase H (from Genzyme) was added to each sample and the samples were incubated at 37°C for 16 h. Gel sample buffer was added and the samples analysed by SDS–PAGE.

Trypsin digestion

Cell lysates and media from metabolically labeled cells were either incubated on ice for 30 min with 50 μg/ml of trypsin [A^-(X31)HA0 only] or at 37°C for 10 min with 10 μg/ml of trypsin [both A^-(X31)HA0 and A^-(Japan)HA0] (trypsin from bovine pancreas, Sigma). Digestion was stopped by adding a 10-fold amount of trypsin inhibitor (from soybean, Sigma), 10 μm chymostatin, 10 μm leupeptin, 10 μm antipain, 10 μm pepstatin and 1 mM PMSF. Controls were treated with protease inhibitors alone. Samples were now immunoprecipitated with polyclonal anti-HA antibodies, analysed by SDS–PAGE under reducing conditions, which dissociated the disulfide bond linking HA1 and HA2.

Inhibition of glycosylation using tunicamycin (TM)

Forty six hours post-infection, cells expressing A^-(X31)HA0 were incubated for 30 min at 37°C with 5 μg/ml of TM in DMEM containing 10 mM HEPES and 10% FCS [stock solution of 5 mg/ml TM in dimethyl sulfoxide (DMSO)]. They were then incubated in methionine-free medium containing TM for another 30 min, pulsed, chased, lysed, applied to gradients

and immunoprecipitated as described above, except that the pulse and chase media containing 5 μg/ml of TM. Control cells were treated identically with DMSO alone.

Acknowledgements

We thank Drs M.-J.Gething and J.Sambrook for the recombinant viruses used, Drs J.J.Skehel, I.A.Wilson and D.G.Bole for monoclonal antibodies, Ann Curley-Whitehouse for help with the photography and Kelsey Martin for critical reading of the manuscript. I.S. thanks members of the Helenius-Mellman Laboratories for helpful discussions, with special thanks to Stella Hurtley for her guidance. The funding was provided by a grant from NIH.

References

Anderson,R.G.W. and Pathak,R.K. (1985) *Cell*, **40**, 635–643.
Bole,D.G., Hendershot,L.M. and Kearney,J.F. (1986) *J. Cell Biol.*, **102**, 1556–1566.
Brand,C.M. and Skehel,J.J. (1972) *Nature*, **238**, 145–147.
Burgess,T.L. and Kelly,R.B. (1989) *Annu. Rev. Cell Biol.*, **3**, 243–293.
Carlin,B.E. and Merlie,J.P. (1986) In Strauss,A.W., Boime,I. and Kreil,G. (eds), *Protein Compartmentalization*. Springer-Verlag, NY, pp. 71–86.
Copeland,C.S., Doms,R.W., Bolzau,E.M., Webster,R.G. and Helenius,A. (1986) *J. Cell Biol.*, **103**, 1179–1191.
Copeland,C., Zimmer,K.-P., Wagner,K.R., Healey,G.A., Mellman,I. and Helenius,A. (1988) *Cell*, **53**, 197–208.
Daniels,R.S., Douglas,A.R., Skehel,J.J. and Wiley,D.C. (1983) *J. Gen. Virol.*, **64**, 1657–1662.
Daniels,R.S., Douglas,A.R., Skehel,J.J., Wiley,D.C., Naeve,C.W., Webster,R.G., Rogers,G.N. and Paulson,J.C. (1984) *Virology*, **138**, 174–177.
Daniels,R.S., Jeffries,S., Yates,P., Schild,G.C., Rogers,G.N., Paulson,J.C., Wharton,S.A., Douglas,A.R., Skehel,J.J. and Wiley,D.C. (1987) *EMBO J.*, **6**, 1459–1465.
Doms,R. and Helenius,A. (1986) *J. Virol.*, **57**, 603–613.
Doms,R.W. and Helenius,A. (1988) In Ohki,S., Flanagan,T.D., Hui,S.W. and Mayhew,E. (eds), *Molecular Mechanisms of Membrane Fusion*. Plenum Press, NY, pp. 385–398.
Doms,R.W., Helenius,A. and White,J. (1985) *J. Biol. Chem.*, **260**, 2973–2981.
Doms,R.W., Keller,D.S., Helenius,A. and Balch,W.E. (1987) *J. Cell Biol.*, **105**, 1957–1968.
Doms,R.W., Ruusala,A., Machamer,C., Helenius,J., Helenius,A. and Rose,J.K. (1988) *J. Cell Biol.*, **107**, 89–99.
Doxsey,S., Helenius,A. and White,J. (1985) *J. Cell Biol.*, **101**, 19–27.
Doyle,C., Sambrook,J. and Gething,M.-J. (1986) *J. Cell Biol.*, **103**, 1193–1204.
Fitting,T. and Kabat,D. (1982) *J. Biol. Chem.*, **257**, 14011–14017.
Gething,M.-J. and Sambrook,J. (1982) *Nature*, **300**, 598–603.
Gething,M.-J. and Sambrook,J. (1989) *Biochem. Soc. Symp.*, **55**, 155–166.
Gething,M.-J., McCammon,K. and Sambrook,J. (1986) *Cell*, **46**, 939–950.
Hurtley,S.M., Bole,D.G., Hoover-Litty,H., Helenius,A. and Copeland,C.S. (1989) *J. Cell Biol.*, **108**, 2117–2126.
Hurtley,S.M. and Helenius,A. (1989) *Annu. Rev. Cell Biol.*, **5**, 277–307.
Klausner,R. (1989) *Cell*, **57**, 703–706.
Kornfeld,R. and Kornfeld,S. (1985) *Annu. Rev. Biochem.*, **54**, 631–664.
Laemmli,U.K. (1970) *Nature*, **227**, 680–685.
Lodish,H.F., Kong,N., Snider,M. and Strous,G.A.M. (1983) *Nature*, **304**, 80–83.
Machamer,C.E. and Rose,J.K. (1988) *J. Biol. Chem.*, **263**, 5955–5960.
Machamer,C.E., Doms,R.W., Bole,G.B., Helenius,A. and Rose,J.K. (1989) in press.
Palade,G.E. (1956) *J. Biophys. Biochem.Cytol.*, **2**, 417–422.
Palade,G.E. (1975) *Science*, **189**, 347–358.
Pfeffer,S.R. and Rothman,J.E. (1987) *Annu. Rev. Biochem.*, **56**, 829–852.
Rose,J.K. and Doms,R.W. (1988) *Annu. Rev. Cell Biol.*, **4**, 257–288.
Schwartz,A.L., Strous,G.J.A.M., Slot,J.W. and Geuze,H.J. (1985) *EMBO J.*, **4**, 899–904.
Skibbens,J.E., Roth,M.G. and Matlin,K.S. (1989) *J. Cell Biol.*, **108**, 821–832.
Strous,G.J. and Lodish,H.F. (1980) *Cell*, **22**, 709–717.
Tooze,J., Kern,H.F., Fuller,S.D. and Howell,K.E. (1989) *J. Cell Biol.*, **109**, 35–50.
Wiley,D.C. and Skehel,J.J. (1987) *Annu. Rev. Biochem.*, **56**, 365–394.
Wilson,I.A., Skehel,J.J. and Wiley,D.C. (1981) *Nature*, **289**, 366–375.
Wilson,I.A., Niman,H.L., Houghten,R.A., Cherenson,A.R., Connolly, M.L. and Lerner,R.A. (1984) *Cell*, **37**, 767–778.
Yewdell,J.W., Yellen,A. and Bächi,T. (1988) *Cell*, **52**, 843–852.

Received on November 2, 1989; revised on December 22, 1989